Virtual time-reversal processing for source localization in shallow water

Tongwei Zhang, Kunde Yang, Yuanliang Ma
Northwestern Polytechnical University, Xi'an 710072, China

***Abstract*-Matched-field processing (MFP) is a forward propagation process that consists of systematically placing a test point source at each point of a search grid, computing the replica vectors on the array and then correlating these replicas with the data from the real source. It will cost much time to calculate all these replica vectors corresponding to the search grids. Time-reversal processing (TRP) is an implementation of MFP where the ocean itself is used to construct the replica field. This paper introduces a virtual time-reversal processing (VTRP) that is implemented electronically at the receiver array and simulates the kind of processing that would be done by an actual TRP during the reciprocal propagation stage. Apart from MFP, VTRP is a back-propagation process which exploits the properties of reciprocity and superposition. Thus, the calculation of the replica surface generated by each virtual source at the corresponding array element location can be speeded up by matrix manipulation. As a result, the localization surface of VTRP can be formed faster than that of MFP. The performance of VTRP for source localization is validated through the numerical simulations.**

I. INTRODUCTION

MFP [1]-[3] deals with target localization by matching the data of the target radiated acoustic field acquired by an array to a model-based replica vector at a test target position. The process consists of systematically placing a test point source at each point of a search grid, computing the acoustic field (replicas) at all the elements of the array and then correlating this modeled field with the data from the real point source whose location is unknown. A search is performed in a region of possible target positions. When the test point source is collocated with the true point source, the correlation will be a maximum. Obviously, it will cost much time to calculate all the replica vectors corresponding to the search grids.

TRP [4]-[8] is a process of retransmitting a received signal in a time-reversed fashion by a source-receiver array. A constructive interference will be created at the original source location due to the medium reciprocity. When TRP is applied to source localization, it is not necessary to send a signal back and forth between source and receiver. Instead, assuming that the acoustic channel is sufficiently stable in time, the retransmission of the temporal dispersed signals in a time reversed fashion will be done inside the computer. In the frequency domain, time reversal is equivalent to phase conjugation. Though this technique is termed as VTRP, the localization surface for source localization should be formed in the frequency domain. It contains the focusing peak which provides the greatest likelihood that the source is present, and also contains ambiguous peaks which are the sidelobes. A passive receive array is used in VTRP instead of a source-receiver array. As its counterpart of TRP, the localization performance of VTRP will depend upon the stability of the propagation channel and the ability of the receiving array to correctly sample the most important features of the acoustic field at the useful frequencies. Both of them work best in a reciprocal acoustic environment, i.e., one in which the Green's function is invariant under exchange of the source and field points. Furthermore, the environmental parameters needed for accurate predictions of acoustic propagation also play an important (crucial) role in VTRP source localization as MFP [9]-[12].

An acoustic signal traveling through the ocean becomes weakened due to various loss mechanisms such as geometrical spreading and attenuation [13]. When time reversal technique applied to source localization, there exists one drawback to this back-propagation approach. Compared with the forward modeling of MFP, it is difficult to re-introduce the attenuated energy in order to arrive at the correct start-up field near the source. From another point of view, because of existence of the sound attenuation, the acoustic intensity close to the "source-receiver" array is much stronger than the focusing peak at the original source location. It means that the focusing peak is only a local maximum around the original source location, but not a global one. If one seeks only a focusing point and not the source strength just like the TRP, this is not a critical complaint.

However, the search region is always from a range close to the receiver array to a far distance just like the matched field localization. The mode-based replica vector is a normalized prediction of the acoustic field on the array due to a test point source located at a candidate position. Thus, the difficulty that the true source peak at the ambiguity surface is masked by the stronger peaks close to the receiver array will not appear in matched field localization. MFP and VTRP are somewhat conceptually similar especially in their mathematical expressions, but differ in their physical implementations.

In order to suppress the stronger peaks close to the receiver array and make the focusing peak to be the global maximum, an appropriate normalization factor should be introduced to the back-propagation field. It means that the acoustic field excited by the virtual source at the array should be normalized. N normalized replica surfaces are calculated numerically from propagation models which corresponding to a point source located at each of the N element positions on the receiving array. The input parameters to the propagation model include the "receiver" position and environmental parameters for the waveguide. The VTRP can be realized by weighting the normalized replica surface by the complex conjugation of the data received on the corresponding element, and then summing up.

Apart from MFP, VTRP is a back-propagation process which exploits the properties of reciprocity and superposition. Thus, the calculation of the replica surface generated by each virtual source at the corresponding array element location can be speeded up by matrix manipulation. As a result, the localization surface of VTRP can be formed much faster than its counterpart of MFP.

II. THEORY BACKGROUND

A. Matched Field Processing

MFP is a forward propagation process that consists of systematically placing a test point source at each point of a search grid, computing the replica vectors on the array and then correlating these replicas with the data from the real source. The replica vector on the array for each candidate position is normalized to unit norm and is denoted by $\mathbf{w}\left(\mathbf{r}_{\text{array}},\mathbf{z}_{\text{array}};r,z\right)=\mathbf{P}(\mathbf{r}_{\text{array}},\mathbf{z}_{\text{array}};r,z)\big/\left|\mathbf{P}(\mathbf{r}_{\text{array}},\mathbf{z}_{\text{array}};r,z)\right|$ here. The vector $\mathbf{r}_{\text{array}}$ reduces to a scalar for vertical line array (VLA), while the vector $\mathbf{z}_{\text{array}}$ reduces to a scalar for horizontal line array (HLA). $\mathbf{P}(\mathbf{r}_{\text{array}},\mathbf{z}_{\text{array}};r,z)$ is the vector whose i th element is the solution to the Helmholtz equation at the i th array element location $\left(r_i,z_i\right)$ for a test source at $\left(r,z\right)$. For a Bartlett matched field processor, the ambiguity function (or surface) at each test point is given by

$$\begin{aligned}S_{\text{MFP}}\left(r,z\right)&=\left|\mathbf{w}^{\text{H}}(\mathbf{r}_{\text{array}},\mathbf{z}_{\text{array}};r,z)\mathbf{d}\left(\mathbf{r}_{\text{array}},\mathbf{z}_{\text{array}};r_s,z_s\right)\right|^2\\&=\mathbf{w}^{\text{H}}(\mathbf{r}_{\text{array}},\mathbf{z}_{\text{array}};r,z)\mathbf{R}\mathbf{w}(\mathbf{r}_{\text{array}},\mathbf{z}_{\text{array}};r,z)\end{aligned}\qquad(1)$$

where $\mathbf{d}\left(\mathbf{r}_{\text{array}},\mathbf{z}_{\text{array}};r_s,z_s\right)$ is a data vector observed on the sensor array, and $\mathbf{R}$ is the data covariance matrix. Superscript $()^{\text{H}}$ denotes the Hermitian operator, or conjugate transpose, of the matrix.

The processor power S_{MFP} is essentially the square of the magnitude of that correlation, and it uses the cross-spectral matrix (CSM) of the array data rather than data directly. When examining the measured acoustic fields, one always observes variations in the amplitude and phase as a function of time. The effects of such variability can be reduced by considering the mean behavior of the CSM of the fields rather than individual samples of the fields themselves.

B. Virtual Time-Reversal Processing

As mentioned previously, the output of Bartlett matched field processor is essentially the square of the magnitude of the correlation between the measured data and the replica data. The output of VTRP, denoted $\mathbf{S}_{\text{VTRM}}\left(\mathbf{r},\mathbf{z}\right)$, at the search region $\left(\mathbf{r},\mathbf{z}\right)$ is given by

$$\mathbf{S}_{\text{VTRP}}\left(\mathbf{r},\mathbf{z}\right)=\left|\sum_{i=1}^{N}d^*\left(r_i,z_i;r_s,z_s\right)\mathbf{w}\left(\mathbf{r},\mathbf{z};r_i,z_i\right)\right|^2\qquad(2)$$

Since the replica surface is normalized, $\mathbf{w}\left(\mathbf{r},\mathbf{z};r_i,z_i\right)=\mathbf{P}\left(\mathbf{r},\mathbf{z};r_i,z_i\right)\big/\left|\mathbf{P}\left(\mathbf{r},\mathbf{z};r_i,z_i\right)\right|$, the superposition of these N surfaces yields a final localization surface whose peak value provides the greatest likelihood that target is present.

In fact, the output of VTRP $S_{\text{VTRP}}\left(r,z\right)$ at each point $\left(r,z\right)$ can also be expressed as

$$S_{\text{VTRP}}\left(r,z\right)=\left|\mathbf{d}^{\text{H}}\left(\mathbf{r}_{\text{array}},\mathbf{z}_{\text{array}};r_s,z_s\right)\mathbf{w}\left(r,z;\mathbf{r}_{\text{array}},\mathbf{z}_{\text{array}}\right)\right|^2\qquad(3)$$

where $\mathbf{d}$, $\mathbf{w}$, $\mathbf{r}_{\text{array}}$ and $\mathbf{z}_{\text{array}}$ are $\left(N\times1\right)$ column vectors. The vector $\mathbf{r}_{\text{array}}$ reduces to a scalar for VLA, while the vector $\mathbf{z}_{\text{array}}$ reduces to a scalar for HLA. However, the physical meaning of VTRP loses its clarity in this expression. Due to the following expression

$$\begin{aligned}&\left|\mathbf{d}^{\text{H}}\left(\mathbf{r}_{\text{array}},\mathbf{z}_{\text{array}};r_s,z_s\right)\mathbf{w}\left(r,z;\mathbf{r}_{\text{array}},\mathbf{z}_{\text{array}}\right)\right|^2\\&=\left|\mathbf{w}^{\text{H}}\left(\mathbf{r}_{\text{array}},\mathbf{z}_{\text{array}};r,z\right)\mathbf{d}\left(\mathbf{r}_{\text{array}},\mathbf{z}_{\text{array}};r_s,z_s\right)\right|^2\end{aligned}\qquad(4)$$

the mathematical expressions of VTRP and MFP are same, $S_{\text{VTRM}}\left(r,z\right)=S_{\text{MFP}}\left(r,z\right)$. However, their physical implementations are different. MFP is a forward propagation process where the forward modeling is required to compute the replica fields at the array. VTRP is a back-propagation process which is done not by the ocean but inside the computer. In VTRP, N normalized replica surfaces are calculated numerically which corresponding to a virtual point source located at each of the N element positions on the receiving array. Due to the utilization of reciprocity and superposition, the VTRP localization surface can be calculated much faster than its counterpart of MFP.

The amplitude and phase of signal fluctuate with time even when stringent efforts are made to fix all controllable parameters. The effects of such variability can be reduced by considering the mean behavior of the fields rather than individual samples of the fields themselves. When using VTRP to process the real data, the data vector $\mathbf{d}\left(\mathbf{r}_{\text{array}},\mathbf{z}_{\text{array}};r_s,z_s\right)$ used for backpropagation can be obtained following the procedure described in Reference [8]. First, a signal matrix $\mathrm{X}\left(\mathbf{r}_{\text{array}},\mathbf{z}_{\text{array}}\right)$ is constructed by gathering multiple signal vectors (or snapshots). Next, using singular value decomposition, the signal matrix can be expressed as the product of a column orthogonal matrix $\mathbf{U}$ whose columns are the left singular vector, a diagonal matrix $\mathbf{\Sigma}$ of singular values, and the transpose of another orthogonal matrix $\mathbf{V}$ whose columns are the right singular vectors. Then, the data vector $\mathbf{d}\left(\mathbf{r}_{\text{array}},\mathbf{z}_{\text{array}};r_s,z_s\right)$ can be obtained from the combination of the left singular vectors with corresponding singular values.

C. Comparison of Execution Time between MFP and VTRP

In this subsection, the execution time between MFP and VTRP is compared and explained. For simplicity, we discuss the case for VLA only. Similarly, the method can also be applied to HLA. In fact, the calculation of acoustic fields occupies the most of the execution time. Therefore, the propagation model used to calculate the acoustic field should be described firstly.

Normal mode method is convenient because it is accurate and computationally efficient. According to the normal mode theory, acoustic pressure field can be expressed in terms of a normal mode expansion. The eigenfunctions and eigenvalues are solutions to the Helmholtz equation under the boundary conditions. In fact, the eigenfunctions satisfy the orthonormality condition $\int_0^\infty \psi_m(z)\psi_n^*(z)/\rho(z)\,dz = \delta_{mn}$, and they also form a complete set $\sum_{m=1}^{M}\psi_m(z_s)\psi_m^*(z)/\rho(z_s) = \delta(z-z_s)$. As a result, the far-field acoustic pressure field is then the weighted sum of the contributions from each mode [13]

$$P(r,z;r_s,z_s) = \frac{i}{\rho(z_s)\sqrt{8\pi(r-r_s)}} e^{-i\pi/4} \sum_{m=1}^{M} \psi_m(z_s)\psi_m(z) \frac{e^{ik_{rm}(r-r_s)}}{\sqrt{k_{rm}}} \tag{5}$$

where eigenfunction ψ_m describes the mode shape for mode m, and k_{rm} is corresponding horizontal wavenumber. M is the number of contribution modes. (r_s, z_s) is the source position in cylindrical coordinates, and (r,z) is the receiver position.

The normal mode program KRAKEN [14] can calculate efficiently and accurately the mode shape functions and horizontal wavenumbers for an ocean acoustic waveguide. Once the geoacoustic parameters are defined and the source frequency is given, the mode shape functions and horizontal wavenumbers can be calculated numerically by a single execution of KRAKEN. Thus, given the amplitudes of the mode shape functions at the source and receiver depth and the corresponding horizontal wavenumbers, the acoustic pressure field due to the source at an arbitrary range (of course at the far-field) can be easily calculated following (5).

For a unit harmonic point source located at (r_s, z_s), we define a vector of receiver depths as $\mathbf{z} = [z_1, z_2, \cdots, z_{ND}]^{\mathrm{T}}$ and a vector of receiver ranges as $\mathbf{r} = [r_1 - r_s, r_2 - r_s, \cdots, r_{NR} - r_s]^{\mathrm{T}}$, so that the acoustic pressure surface $\mathbf{P}(\mathbf{r},\mathbf{z};r_s,z_s)$ (or vector $\mathbf{P}(r,\mathbf{z};r_s,z_s)$ corresponding to one receiver range) which can be expressed in (5) also takes the form

$$\begin{aligned}\mathbf{P}(\mathbf{r},\mathbf{z};r_s,z_s) = i \times e^{-i\pi/4}\boldsymbol{\Psi}(\mathbf{z})\,\mathrm{diag}\left(\boldsymbol{\Psi}(z_s)\right)\mathrm{diag}(1/\sqrt{\mathbf{K}}) \times \\ \exp(i\mathbf{K}\mathbf{r}^{\mathrm{T}})\,\mathrm{diag}(1/\sqrt{8\pi\mathbf{r}})\end{aligned} \tag{6}$$

where $\mathbf{K}$ is a vector of horizontal wavenumbers, $\mathbf{K} = [k_1, k_2, \cdots, k_M]^{\mathrm{T}}$, $\boldsymbol{\Psi}(z_s)$ is a vector of eigenfunction values at source depth z_s, $\boldsymbol{\Psi}(z_s) = [\psi_1(z_s), \psi_2(z_s), \cdots, \psi_M(z_s)]^{\mathrm{T}}$, and $\boldsymbol{\Psi}(\mathbf{z})$ is a matrix of eigenfunction values at receiver depths $\mathbf{z}$, $\boldsymbol{\Psi}(\mathbf{z}) = [\psi_1(\mathbf{z}), \psi_2(\mathbf{z}), \cdots, \psi_M(\mathbf{z})]$.

Once the numbers of search grids and array elements are chosen, the numbers of evaluation of (5) for MFP and VTRP are fixed, and they are same. For example, the search region is divided into $ND \times NR$ grids, and the array consists of N elements, both the MFP and VTRP will evaluate $ND \times NR \times N$ times of (5). Though the numbers of evaluation of (5) for MFP and VTRP are the same, their calculation times are different because the calculation can be speeded up by matrix manipulation following (6). The processes of MFP and VTRP are shown schematically in Fig. 1.

MFP is a forward propagation process. In this process, a test point source is systematically placed at each point of a search grid. Then the N-dimensional replica vector $\mathbf{P}(r_{\text{array}}, \mathbf{z}_{\text{array}}; r, z)$ at the array is computed as shown in Fig. 1(a). It should be noted that only a N-dimensional column replica vector at the array is calculated for a test point source. Let's suppose that the calculation of the N-dimensional replica vector $\mathbf{P}(r_{\text{array}}, \mathbf{z}_{\text{array}}; r, z)$ will cost t_{MFP} seconds. For a search region of $ND \times NR$ grids, we will run $ND \times NR$ times to calculate all these replica vectors at the array. Thus, it will cost $ND \times NR \times \mathrm{t}_{\text{MFP}}$ seconds, denotes T_{MFP}.

Apart from MFP, VTRP is a back-propagation process which exploits the properties of reciprocity and superposition. It is assumed that there are N virtual point sources located at each of the N element positions on the receiving array. Each

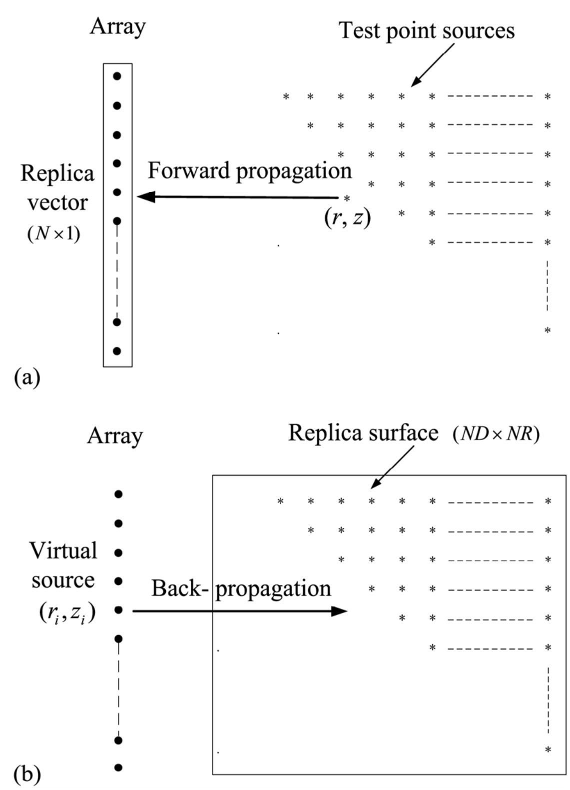

Figure 1. Schematic of the procedure of the processor for VLA: (a) MFP, and (b) VTRP.

virtual point source (r_i, z_i) generates a replica surface $\mathbf{P}(\mathbf{r}, \mathbf{z}; r_i, z_i)$ which corresponding to a search region of $ND \times NR$ grids as shown in Fig. 1(b). Let's suppose that the calculation of the $ND \times NR$ -dimensional replica matrix (surface) $\mathbf{P}(\mathbf{r}, \mathbf{z}; r_i, z_i)$ will cost $\mathrm{t_{VTRP}}$ seconds. Therefore, the generation of N replica surfaces corresponding to the N virtual point sources will cost $N \times \mathrm{t_{VTRP}}$ seconds, denotes $\mathrm{T_{VTRP}}$.

As mentioned previously, the forward propagation MFP costs $\mathrm{T_{MFP}}$ seconds to calculate all the acoustic fields while the back-propagation VTRP costs $\mathrm{T_{VTRP}}$ seconds. Thus, MFP calculation time is $\mathrm{T_{MFP}}/\mathrm{T_{VTRP}}$ times larger than that of VTRP. If we calculate the acoustic fields point by point following (5), i.e., using loops, the calculation time of $ND \times NR$ replica surface in VTRP is much larger than that of $N \times 1$ vector in MFP, about $ND \times NR/N$ times. However, they are calculated through matrix manipulation following (6), thus $\mathrm{t_{VTRP}}$ is only several times larger than $\mathrm{t_{MFP}}$. Therefore, MFP calculation time $\mathrm{T_{MFP}}$ is much larger than $\mathrm{T_{VTRP}}$ of VTRP, about several dozen times. For example, if the search region is divided into 51 rows and 301 columns, and the array consists of 48 elements, thus $ND \times NR/N = 51 \times 301/48 \approx 320$; while $\mathrm{t_{VTRP}}/\mathrm{t_{MFP}} \approx 8$ which is obtained from later simulation, thus $\dfrac{\mathrm{T_{MFP}}}{\mathrm{T_{VTRP}}} = \dfrac{ND \times NR \times \mathrm{t_{MFP}}}{N \times \mathrm{t_{VTRP}}} \approx 40$.

III. Numerical Simulation

A. Simulation Conditions

Simulated data are generated for simulation experiment. The ocean model must be defined before the acoustic propagation can be modeled and the acoustic fields are computed. Fig. 2 shows the range-independent shallow-water channel used for simulations. It consists of an ocean layer overlying a thin sediment layer and a bottom layer. The sound speed in the water-column is modeled as a summer profile with an almost isovelocity layer extending to 60 m and a strong thermocline spanning 60-80 m depth. The ocean surface is treated as a flat pressure-release surface.

The point source is narrow-band at a frequency of 170 Hz. It locates at 5.5 km in range and 76 m in depth. It is assumed that the whole environment is not changed with time. Thus the sound channel is reciprocal. For simplicity, the ambient noise is ignored. A search region over source range and depth is performed from 10 to 110 m in depth and from 1 to 10 km in range. The localization surface is normalized so that the peak value is 0 dB. The location of the maximum (0 dB) of the localization surface is used as the source location parameter estimate.

In order to quantify the localization performance, the output signal to interference noise ratio (SINR) [15] is used. In the following simulations, once the maximum of the ambiguity surface is within the neighborhood (±500m in range and ±10m

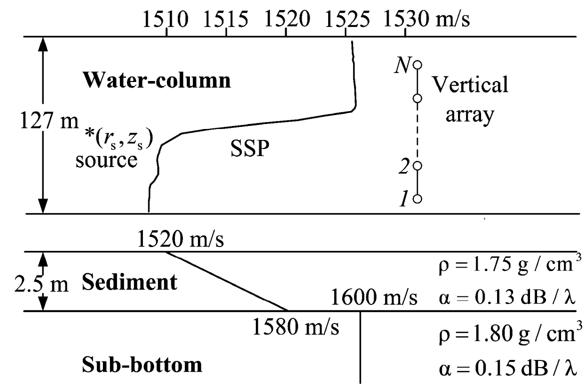

Figure 2. Range-independent shallow-water sound channel with geometric and environmental parameters for Mediterranean environment north of Elba. The VLA spans the water column from 18.7 to 112.7 m with 2 m element spacing.

in depth) of the true source location, then the localization is correct, and vice versa. The SINR is defined as the maximum output signal (normalized to 0 dB) minuses the 75th percentile of the normalized localization surface powers after sorting in ascending order (100th percentile means the peak of localization surface). Once the localization failed, the SINR is meaningless, and let it be 0 dB.

B. Simulation Results

Most underwater acoustics experiments have been performed using a VLA. The VLA has often been the preferred tool of research due to its ability to sample the spatial variability of the acoustic field with respect to depth in the water. Typically for a fixed location experiment, the vertical line array can be deployed from an anchored vessel and vertically aligned by a weight, or moored from the ocean floor and suspended by a float.

The VLA consists of 48 elements spanning the water column from 18.7 to 112.7 m with 2 m interelement spacing. The range-depth search grid is 30×2 m. The localization performance of MFP and VTRP are compared, as shown in Fig. 3. Fig. 3(a) is the case of Bartlett matched field processor. The source is correctly localized, and its output SINR is 11.7815 dB. Fig. 3(b) shows the localization surface formed by VTRP. The focused peak illustrates that the source localization is correct, and its output SINR is also 11.7815 dB. As discussed in Sec. II, the mathematical expressions of VTRP and MFP are same, so their localization performances are identical. However, their physical implementations are different. MFP is a forward propagation process while VTRP is a back-propagation one. Furthermore, VTRP utilizes the property of reciprocity and superposition, so its localization surface can be formed much faster than MFP.

Unlike the DSP chipset, when we run a program on the PC, the Operation System and other required software will occupy the memory, and their occupied time and space are not absolutely the same. Thus the execution time of the same program on the PC is not a fixed value but has minor fluctuation. Fig. 4 shows the execution time of VTRP and MFP at different execution number. It confirms that the execution time fluctuates markedly. Thus, the time averaged over 50 executions is used to represent the execution time. The average execution times of VTRP and MFP are 0.2919 and 11.5538 s, respectively. It means that VTRP proceeds about 40 times faster than MFP.

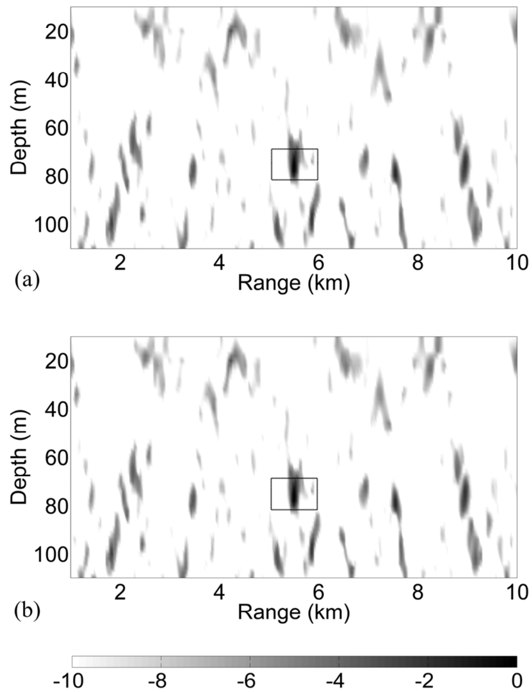

Figure 3. Range/depth localization surfaces obtained in the scenario of Fig.2 for a VLA with simulated data and the true source range/depth of 5.5 km/76 m: (a) MFP and (b) VTRP.

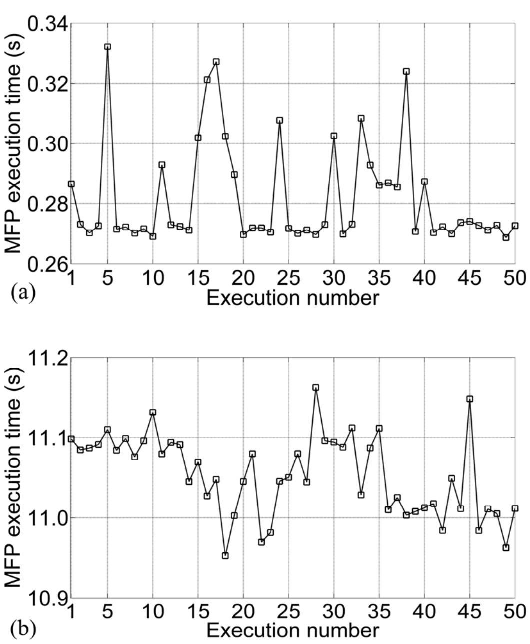

Figure 4. The execution time for different execution number: (a) VTRP and (b) MFP.

IV. CONCLUSIONS

In the forward propagation MFP, the replica vectors corresponding to the search grids should be calculated one by one. Of course, it is laborious and time-consuming. In this paper, the concept of VTRP for source localization is introduced. Apart from MFP, VTRP is a back-propagation process which exploits the properties of reciprocity and superposition as its counterpart of TRP. In VTRP, N normalized replica surfaces are calculated numerically which corresponding to a virtual source located at each of the N element positions on the receiving array. Thus, the calculation of the replica surface corresponding to each virtual source located at the array can be speeded up by matrix manipulation. Simulation results in shallow-water show that VRTP can be used for vertical line array. Compared to MFP, VRTP can achieve same localization performance while costs much less execution time.

ACKNOWLEDGMENT

The work was supported by the National Natural Science Foundation of China (Grant Nos. 10774119), the program for New Century Excellent Talents in University (NCET-08-0455), the Natural Science Foundation of Shaanxi province, China (Grant No. SJ08F07), the Foundation of National Laboratory of Acoustics, and the NPU Foundation for Fundamental Research.

REFERENCES

[1] A. B. Baggeroer, W. A. Kuperman, and P. N. Mikhalevsky, "An overview of matched field methods in ocean acoustics," *IEEE J. Ocean. Eng.* vol.18, no.4, pp.401-422 Oct. 1993.

[2] A. Tolstoy, *Matched field processing for underwater acoustics.* Singapore: World Scientific, 1993.

[3] K. D. Yang, *Matched-Field Processing for Underwater Acoustic Array Signals.* Xi'an: Northwestern Polytechnical University Press, 2008.

[4] D. R. Jackson, and D. R. Dowling, "Phase conjugation in underwater acoustics," *J. Acoust. Soc. Am.* vol.89, no.1, pp.171-181 Jan. 1991.

[5] D. R. Dowling, and D. R. Jackson, "Narrow-band performance of phase conjugate arrays in dynamic random media," *J. Acoust. Soc. Am.* vol. 91, no. 6, pp.3257-3277 Jun. 1992.

[6] W. A. Kuperman, W. S. Hodgkiss, H. C. Song, T. Akal, C. Ferla, and D. R. Jackson, "Phase conjugation in the ocean: Experimental demonstration of an acoustic time-reversal mirror," *J. Acoust. Soc. Am.* vol. 103, no.1, pp. 25-40 Jan. 1998.

[7] M. Fink, D. Cassereau, A. Derode, C. Prada, P. Roux, Mickael Tanter, J. L. Thomas, and F. Wu, "Time-reversed acoustics," *Rep. Prog. Phys.* vol. 63, no.12, pp.1933-1995 Dec. 2000.

[8] S. Kim, W. A. Kuperman, W. S. Hodgkiss, H. C. Song, G. G. Edelmann, and T. Akal, "Robust time reversal focusing in the ocean," *J. Acoust. Soc. Am.* vol. 114, no. 1, pp.145-157 Jul. 2003.

[9] R. M. Hamson, and R. M. Heitmeyer, "Environmental and system effects on source localization in shallow water by the matched-field processing of a vertical array," *J. Acoust. Soc. Am.* vol. 86, no.5, pp.1950-1959 Nov. 1989.

[10] S. M. Jesus, "Normal-mode matching localization in shallow water: Environmental and system effects," *J. Acoust. Soc. Am.* vol. 90, no. 4, pp. 2034-2041 Oct. 1991.

[11] J. Tabrikian, and J. L. Krolik, "Robust maximum-likelihood source localization in an uncertain shallow-water waveguide," *J. Acoust. Soc. Am.* vol. 101, no. 1, pp. 241-249 Jan. 1997.

[12] C. Debever, and W. A. Kuperman, "Robust matched-field processing using a coherent broadband white noise constraint processor," *J. Acoust. Soc. Am.* vol. 122, no. 4, pp. 1979-1986 Oct. 2007.

[13] F. B. Jensen, W. A. Kuperman, M. B. Porter, and H. Schmidt, *Computational Ocean Acoustics*. New York: AIP Press, 1994.
[14] M. B. Porter, "The KRAKEN normal mode program," Technical Report, SACLANT Undersea Research Center, La Spezia, Italy, 1991.
[15] K. D. Yang, and Y. L. Ma, "Robust adaptive matched field processing with sector eigenvector constraints", *Chinese Journal of Acoustics* vol. 25, no. 3, pp. 243-257 2006.